Structure of the Skeletal Muscle Calcium Release Channel Activated with Ca^{2+} and AMP-PCP

I. I. Serysheva,*# M. Schatz,§¶ M. van Heel,¶ W. Chiu,*# and S. L. Hamilton*

*Department of Molecular Physiology and Biophysics and #Verna and Marrs McLean Department of Biochemistry, Baylor College of Medicine, Houston, Texas 77030 USA; §Image Science Software GmbH, D-10711 Berlin, Germany; and ¶Department of Biochemistry, Imperial College of Science, Medicine and Technology, London SW7 2AY, England

ABSTRACT The functional state of the skeletal muscle Ca^{2+} release channel is modulated by a number of endogenous molecules during excitation-contraction. Using electron cryomicroscopy and angular reconstitution techniques, we determined the three-dimensional (3D) structure of the skeletal muscle Ca^{2+} release channel activated by a nonhydrolyzable analog of ATP in the presence of Ca^{2+}. These ligands together produce almost maximum activation of the channel and drive the channel population toward a predominately open state. The resulting 30-Å 3D reconstruction reveals long-range conformational changes in the cytoplasmic region that might affect the interaction of the Ca^{2+} release channel with the t-tubule voltage sensor. In addition, a central opening and mass movements, detected in the transmembrane domain of both the Ca^{2+}- and the Ca^{2+}/nucleotide-activated channels, suggest a mechanism for channel opening similar to opening-closing of the iris in a camera diaphragm.

INTRODUCTION

Excitation-contraction (E-C) coupling is the process in muscle that links depolarization of the plasmalemma membrane to Ca^{2+} release from the sarcoplasmic reticulum (SR), the main source of Ca^{2+} in muscle. The release of Ca^{2+} occurs via the cation-selective, ligand-regulated Ca^{2+} release channel located in the junctional membrane of the SR in response to signals arising from the voltage-dependent Ca^{2+} channels (dihydropyridine receptors) in the t-tubule. The increase in the intracellular Ca^{2+} concentration initiates muscle contraction. Thus the Ca^{2+} release channel plays a critical role in the regulation of muscle contraction. The native form of the skeletal muscle Ca^{2+} release channel is a tetramer (Lai et al., 1989) with a subunit molecular mass of 565 kDa (Takeshima et al., 1989; Zorzato et al., 1990). Because the 12-kDa FK506-binding protein, FKBP12, is considered an integral part of the functional Ca^{2+} release channel (Jayaraman et al., 1992; Timerman et al., 1993, 1995), the entire channel assembly represents a heterooligomer with a molecular mass of over 2.3 MDa.

The skeletal muscle Ca^{2+} release channel probably exists in several distinct functional states during the excitation-contraction coupling process. The functional channel transitions are regulated by a wide variety of endogenous molecules and pharmacological modifiers (see reviews: Coronado et al., 1994; Fleischer and Inui, 1989; Meissner, 1994; Ogawa, 1994). It has been suggested that the Ca^{2+} release channel undergoes global conformational changes in response to the binding of modulators (Ikemoto et al., 1985; Kang et al., 1992; Ohkusa et al., 1991; Orlova et al., 1996). The plant neutral alkaloid, ryanodine, binds preferentially to the open state of the Ca^{2+} release channel (Chu et al., 1990; Holmberg and Williams, 1990; McGrew et al., 1989; Meissner, 1986a; Pessah and Zimanyi, 1991) and is, therefore, frequently used as a probe of the functional state of the channel. Ryanodine alters the conductance and gating properties of the channel, and the nature of the functional effect is dependent on ryanodine concentration. At submicromolar concentrations, ryanodine binds to one or more high-affinity sites and locks the channel in an open, reduced-conductance state (Diaz-Munoz et al., 1990; Meissner, 1986b; Rousseau et al., 1987; Wang et al., 1993). Higher concentrations of ryanodine (μM range) close the channel (Nagasaki and Fleischer, 1988). The molecular mechanism by which the binding of ryanodine alters channel activity is still unknown.

In our previous studies using electron cryomicroscopy and angular reconstitution techniques (Orlova et al., 1996; Serysheva et al., 1995), we were able to detect global conformational changes in both the transmembrane and the cytoplasmic regions of the Ca^{2+} release channel upon the functional switching between closed and open states of the channel in the presence of Ca^{2+} and ryanodine. Thus the alterations in the gating properties of the Ca^{2+} release channel may arise from the structural modifications observed in the presence of ryanodine. Ryanodine may act either by inducing or stabilizing conformational changes in the sarcoplasmic reticulum Ca^{2+} release channel that prevent it from closing (Pessah and Zimanyi, 1991; Tinker et al., 1996). However, the physiological relevance of conformational changes in the three-dimensional structure of the Ca^{2+} release channel induced by ryanodine is questionable. The Ca^{2+} release channel normally does not assume a state resembling the ryanodine-modified channel. To examine the structure of the open channel under conditions more closely approximating physiological conditions, we have

Received for publication 17 March 1999 and in final form 23 June 1999.

Address reprint requests to Dr. Susan L. Hamilton, Department of Molecular Physiology and Biophysics, Baylor College of Medicine, One Baylor Plaza, Houston, TX 77030. Tel.: 713-798-5704; Fax: 713-798-5441; E-mail: susanh@bcm.tmc.edu.

© 1999 by the Biophysical Society

0006-3495/99/10/1936/09 $2.00

now determined the 3D structure of the skeletal muscle Ca^{2+} release channel activated in the presence of Ca^{2+} and in the presence of Ca^{2+} and the nonhydrolyzable analog of ATP, AMP-PCP.

Ca^{2+} and adenine nucleotides are considered to be important modulators of the SR Ca^{2+} release channels. Skeletal muscle Ca^{2+} release channels open transiently in the presence of micromolar Ca^{2+} (Meissner et al., 1986; Meissner and el-Hashem, 1992; Meissner and Henderson, 1987). The probability (P_o) of the channel opening is increased by a rise in the free Ca^{2+} concentration within the nM to μM range (Copello et al., 1997; Smith et al., 1986) and reaches maximum values of ~0.6 at 100–200 μM Ca^{2+} (Rousseau et al., 1992; Smith et al., 1986, 1988). Elevation of the Ca^{2+} concentration at the cytosolic face of the channel above ~200 μM produces a decrease in channel opening (Ma et al., 1988; Meissner et al., 1986; Meissner and Henderson, 1987; Smith et al., 1986, 1988). Thus Ca^{2+} alone is not sufficient to fully activate the channel. Millimolar ATP in the presence of micromolar Ca^{2+} appears to efficiently activate the SR Ca^{2+} release channel and produces channel activation with a P_o near unity (Smith et al., 1986, 1988). Under these conditions, the open-channel form, exhibiting a full conductance characteristic for the native channel, is predominant. Using these conditions we can drive the channel to the open state and trap it there by rapid freezing.

Here we present the 3D reconstruction of the skeletal muscle Ca^{2+} release channel in two functional states: 1) the "fully open state" in the presence of 1 mM AMP-PCP and 100 μM Ca^{2+} and 2) the "transiently open state" in the presence of 100 μM Ca^{2+} only. These reconstructions are compared to a new refined reconstruction of the "closed state" channel, obtained in the absence of Ca^{2+}, and our previously published "ryanodine-modified open state," obtained in the presence of Ca^{2+} and ryanodine (Orlova et al., 1996).

MATERIALS AND METHODS

Protein purification

The Ca^{2+} release channel protein was purified from skeletal muscle SR membranes as previously described, with some modifications (Hawkes et al., 1989). Briefly, the sarcoplasmic reticulum membrane fraction enriched in [^{3}H]ryanodine binding was solubilized with 2% 3-[(3-cholamidopropyl)dimethylammonio]-1-propane sulfonate (CHAPS) in 50 mM 3-(*N*-morpholino)propanesulfonic acid (MOPS) (pH 7.4) containing 185 mM NaCl, 2 mM dithiothreitol (DTT), and 0.1 M EGTA. The solubilized channel protein was then purified by a two-step procedure: ion-exchange chromatography on a DEAE-Trisacryl M column followed by centrifugation through a 5–20% sucrose density gradient, and then further concentrated on a DEAE-Trisacryl M column. The functional integrity of the purified protein was confirmed by performing binding with [^{3}H]ryanodine and by reconstitution of the purified channel into planar lipid bilayer. Protease inhibitors (1 μg/ml leupeptin, 2 μg/ml pepstatin, 0.2 mM phenylmethylsulfonyl fluoride, 0.2 mM aminobenzamidine, 2 μg/ml aprotinin) were used throughout the protein isolation. Because repeated freeze-thawing is detrimental to the protein, the purified Ca^{2+} release channel was either used for electron microscopy immediately after preparation or stored in small alliquots at −80°C in 10 mM MOPS (pH 7.4) containing 5% sucrose, 300 mM KCl, 1 mM DTT, and 0.4% CHAPS, and thawed only once before freezing on the grid.

Sample preparation and electron cryomicroscopy

To maintain the Ca^{2+}-release channel in specific functional states, the channel protein was vitrified under different buffer conditions. The closed-state channel was obtained by depletion of Ca^{2+} with 1 mM EGTA (free $Ca^{2+} < 10$ nM) as described earlier (Serysheva et al., 1995). It has been shown that the Ca^{2+} dependence of [^{3}H]ryanodine binding to the channel protein has a bell shape with an optimum at 10–100 μM Ca^{2+} (Lai et al., 1989; McGrew et al., 1989; Meissner, 1986a; Wang et al., 1993). For this reason we have chosen 100 μM Ca^{2+} for our studies. The fully open channel conformations were obtained by activation of the Ca^{2+} release channel with 1 mM AMP-PCP, in the presence of 100 μM Ca^{2+} (fully open channel), and in the presence of 100 μM Ca^{2+} alone (transiently open state channel). The protein was embedded in a thin layer of vitreous ice on a holey carbon grid covered with a thin continuous carbon film.

The frozen-hydrated specimen was transferred into a JEOL1200 microscope, using a GATAN cryoholder and cryotransfer system and imaged at −160°C under minimal-dose conditions (5–7 e/Å^2) at 100 kV accelerating voltage and at a nominal magnification of 30,000 or 40,000. The images were recorded on Kodak SO-63 film.

Image processing and 3D reconstruction

The quality and the defocus of the electron micrographs of the Ca^{2+} release channel were evaluated by performing fast Fourier transform of digitized micrographs (Zhou et al., 1996). The micrographs were scanned on a Perkin-Elmer 1010M microdensitometer or on a Zeiss Phodis scanner with a step size of 6.67 Å/pixel or 3.5 Å/pixel, respectively. On the basis of the contrast transfer function ring positions in computed diffraction patterns (Zhou et al., 1994), the defocus of the images used for processing was estimated to be in the range of ~2.0–2.4 μm, with the corresponding first zero at 1/30 Å^{-1} - 1/26 Å^{-1}. The 3D reconstruction was determined only to the first zero in the contrast transfer function; thus no contrast transfer function correction was applied.

For each sample preparation the best (typically seven to eight) electron micrographs with similar defocus values were processed using the IMAGIC-5 software system (van Heel et al., 1996), essentially as described earlier (Schatz et al., 1995; Serysheva et al., 1995). Channel particles were selected interactively from the micrographs and boxed out into individual images. The molecular images were automatically sorted into homogeneous groups and averaged into characteristic views (class averages). Several iterations of particle image alignment followed by multivariate statistical analysis classification were performed on the individual images data set, using either the class averages or the reprojections from a newly determined 3D map as reference images. The final 3D reconstruction of the Ca^{2+} release channel, activated with AMP-PCP in the presence of μM Ca^{2+}, was computed with 150 characteristic views containing ~4000 of the 6000 original molecular images. One hundred fifty-seven class averages (~3500 particle images from a total of 5800) and 160 class averages (~4000 particle images of 6400) were used in our final 3D reconstructions of the closed channel and of the transiently open channel, respectively. The internal quality of class averages was measured by their compactness in terms of intraclass variance per class member (van Heel, 1989) and by the statistical resolution attained in the class average, using the S-image criterion (Sass et al., 1989). The best results were obtained with an average class size of ~20 molecular images. The quality of the Euler angle assignment for a given class average is measured by the standard deviation of all symmetry-related peaks in the Cross-Sinogram correlation functions of the class average with respect to all of the anchor set images (Schatz et al., 1995; Serysheva et al., 1995). The fit of each class average to the 3D reconstruction is also measured by the differences between the class average used as input in the 3D reconstruction and the corresponding

reprojection of the reconstruction. All of these criteria were used to discard "bad" class averages before the final reconstruction was calculated.

Resolution and visualization of maps

To assess the resolution of the reconstructions, each data set was divided into two equivalent groups, which led to two independent reconstructions. These reconstructions were compared by the Fourier shell correlation method (Orlova et al., 1997; van Heel and Harauz, 1986). To account for the C4 pointgroup symmetry constraints imposed on the 3D reconstruction, the 3σ threshold function was here multiplied by $\sqrt{4}$ (Orlova et al., 1997).

The 3D maps of the Ca^{2+} release channel are rendered at the threshold level chosen to include a volume corresponding a channel molecular mass of ~2.4 MDa, assuming a protein density of 1.35 g/cm^3. To test the statistical significance of features in 3D reconstructions, we also rendered maps at a variety of contour levels, assuming that if a feature is not statistically relevant, its appearance should strongly depend on the chosen threshold value. For the purpose of comparison, the 3D maps were scaled using EMAN Software (Ludtke et al., 1999).

RESULTS

Electron cryomicroscopy of the Ca^{2+} release channel and image analysis

Fig. 1 shows an electron micrograph of ice-embedded Ca^{2+} release channels exhibiting random orientations in the presence of 1 mM AMP-PCP and 100 μM Ca^{2+}. Many rare oblique or side views of the channel particles cannot be visually recognized in the unprocessed data. Only after an iterative procedure of image processing (Schatz et al., 1995) did these rare views, important for attaining an isotropic resolution in the final 3D reconstruction, become statistically significant. The analysis confirmed a sufficiently random distribution of orientations of the channel particles in three, large-population data sets: closed channels in the presence of 1 mM EGTA, transiently open channels (100 μM Ca^{2+}), and channels opened in the presence of 1 mM AMP-PCP and 100 μM Ca^{2+}. The Euler angle distributions of the final class averages used for the 3D reconstructions of the closed, transiently open, and Ca^{2+}/nucleotide-activated channels are shown in Fig. 2. The Euler angle distributions within the asymmetrical triangle for the fourfold rotational symmetry are almost uniform and quite similar for the three different samples studied here. The presence of preferred views, such as the fourfold symmetrical view from the SR toward the t-tubule membrane ($\beta = \sim 180°$), is not a problem, because they are automatically down-weighted by the reconstruction procedure. It is important, however, that the data set be large enough to provide a statistically significant number of each of the rare views of the protein.

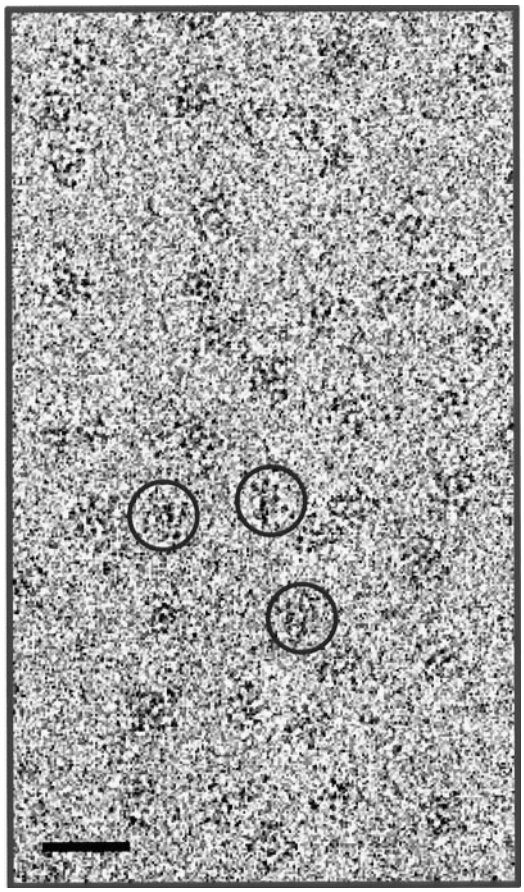

FIGURE 1 Part of a typical electron micrograph of Ca^{2+} release channel particles embedded in a thin layer of vitreous ice in the presence of 100 μM Ca^{2+} and 1 mM AMP-PCP. A few particles in different orientations are marked with circles. Bar, 500 Å.

Overall features in the 3D reconstructions

In Fig. 3 the surface representation of the 3D reconstructions of the closed channel, the transiently open and the fully opened channels, are shown side by side. The reproducible resolution is 30 Å for all three reconstructions of the Ca^{2+} release channel, as determined by Fourier shell correlation method (Orlova et al., 1997; van Heel and Harauz, 1986). The characteristic mushroom shape of the channel consists of a large square cytoplasmic (CY) domain (270 × 270 Å) with clamp-shaped (*C*) subdomains, located at the corners of the CY region interconnected by "handle" (*H*) subdomains (Fig. 3). This domain is likely to be in the cytoplasm and may be involved in interactions with the t-tubule membrane. The central opening of ~50 Å diameter can be seen in the CY region in all three maps. The mushroom stem is formed by the small square transmembrane (TM) region (120 × 120 Å) facing the SR lumen and connected to the CY region by four column subdomains. In these new reconstructions the channels are ~190 Å high. The cytoplasmic and transmembrane domains are rotated by ~40° with respect to each other, as was shown in earlier studies (Orlova et al., 1996; Radermacher et al., 1994; Serysheva et al., 1995).

Our new map of the closed-state Ca^{2+} release channel confirms all basic features seen in our previous reconstruction (Serysheva et al., 1995), but the structural details are now better defined. The transmembrane domain of the new closed-channel reconstruction displays a more apparent handedness than seen in the earlier map. The indentures on the sides of the square TM domain are similar to those of the

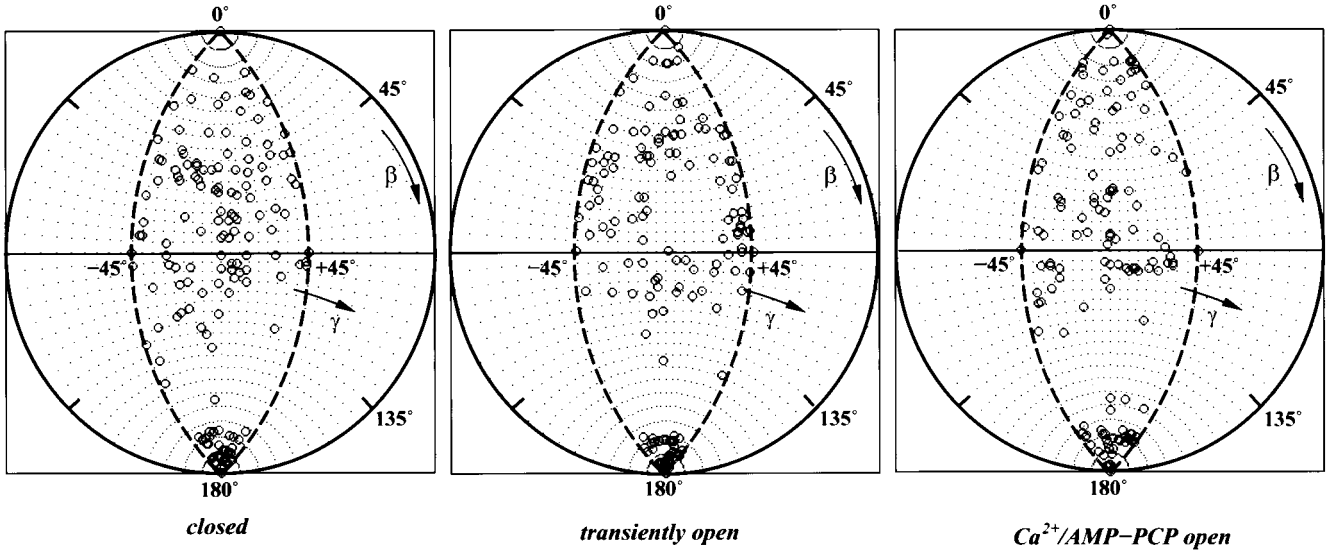

FIGURE 2 Euler angle distributions of the characteristic views used for calculating the 3D maps of the Ca^{2+} release channel in its closed, transiently open, and Ca^{2+}/nucleotide open states. Each class-average orientation is depicted by a point in the asymmetrical "triangle," which, for a fourfold symmetrical protein, spans a quarter of the unit sphere, with β ranging from 0° to 180° and γ ranging from −45° to +45°. Because the projection directions north of the equator are equivalent to their mirror images south of the equator, the overall coverage of the asymmetrical triangle by characteristic views is complete.

open channels. The absence of the central cavity in the TM domain is characteristic of the closed (nonconducting) channel conformation. The clamp-shaped (*C*) subdomains are also better resolved in the new map of the closed channel. Although the height of the closed channel remained the same (~190 Å), the finger-like subdomains of the "clamps" pointing toward the t-tubule are distinct and are separated from the neighboring subdomains by more pronounced clefts. The tips of the fingerlike domains of the "clamp" are tilted inward.

Ca^{2+}- and Ca^{2+}/AMP-PCP-induced changes in channel structure

The 3D maps of the transiently open and the fully open channels (Fig. 3) exhibit both similarities and differences compared to the closed channel. The changes in the 3D channel structure in the transiently open and the fully open channels are most pronounced in the transmembrane region, where the putative ion-conducting pathway is located. The small central opening with a ~7-Å diameter on the lumenal side of the transmembrane domain is revealed in the transiently open channel (Fig. 3). The central opening in the reconstruction of the Ca^{2+}/AMP-PCP open channel is not readily seen in the surface renderings at the chosen threshold level, corresponding to 2.4 MDa and used for displaying all other maps. However, the funnel shape of the TM domain around its center is quite obvious and indicates that the mass rearrangement in the TM domain is similar to that in the transiently open channel. This is best visualized in Fig. 3 *c*, where reconstructions are dissected along the fourfold axis of the channel, to show the internal features of the Ca^{2+} release channel under different conditions. A pronounced mass depletion from the center of the TM region can be seen in both reconstructions of the transiently and the fully open channels.

The clamp-shaped subdomains at the four corners of the CY region in the Ca^{2+}/nucleotide open channel are in an open conformation, similar to that previously seen with the ryanodine-modified open channel (Orlova et al., 1996). In contrast, the clamp-shaped domains in the transiently open channel appear in a more closed conformation similar to the "clamps" in the closed channel (Fig. 3, *a* and *b*). In addition, the finger-like subdomains in the open "clamps" are slightly straightened toward the surface of the t-tubule membrane (Fig. 3 *c*).

Analysis of movements in TM domain upon channel activation

Fig. 4 represents surface renderings of the TM domains, computationally extracted from the reconstructions of the channel in closed, transiently open, Ca^{2+}/AMP-PCP open, and ryanodine-modified open states. In our structural analysis, to reveal the strongest densities within the reconstructions and to evaluate the statistical significance of observed structural differences between reconstructions of the Ca^{2+} release channel in different functional states, maps were displayed at different contour levels. The features, determined in all three maps of the Ca^{2+} release channel, are not strongly dependent on the chosen threshold value in the range of 2.2–2.7 MDa. Fig. 4 represents the TM domains of

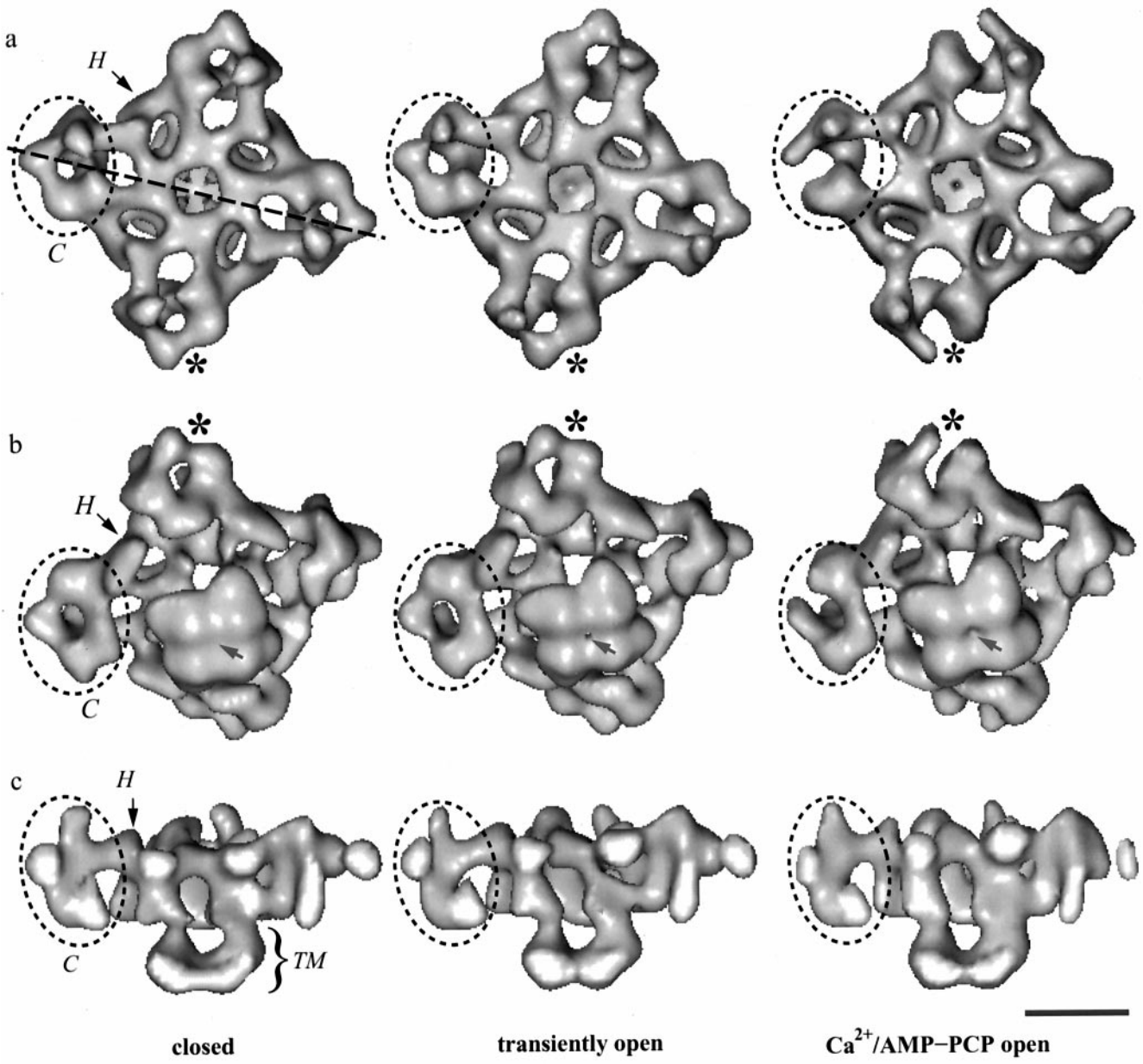

FIGURE 3 Surface representation of the 3D reconstructions of the Ca^{2+} release channel in three functional states: closed (Ca^{2+} depleted with 1 mM EGTA, free Ca^{2+} less than 10 nM), transiently open (in the presence of 100 μM Ca^{2+}), and fully open (in the presence of 1 mM AMP-PCP and 100 μM Ca^{2+}). (*a*) Top views from the cytoplasm toward the SR membrane show the cytoplasmic face of the channel. (*b*) Tilted views from the SR lumen toward the cytoplasm with the cytoplasmic side facing upward. (*c*) Views of reconstructions cut open through the fourfold axis along the diagonal of the cytoplasmic domain. The dashed line in a top view of the closed map (*a*) indicates the direction of sectioning. Note the differences in "clamp-shaped" (*C*) domains (*asterisk*) and the presence and absence of the central opening in the TM domains (*arrows*). Bar, 100 Å.

the reconstructions contoured at two different threshold levels. The TM domain portions of the reconstructions, contoured at a molecular volume corresponding to 2.4 MDa for the entire channel, are shown as transparent surfaces in Fig. 4. The strongest densities (25% of nominal volume) within the TM domains, shown in a solid yellow color, have a beanlike shape and exhibit different orientations with respect to the channel fourfold axis. The beanlike subdomains in the open channel (Fig. 4) are oriented more parallel to the channel axis than they appear in the closed-state channel (Fig. 4), and their distal parts, apparently exposed to the SR lumen, are drawn away from the central axis. These movements of the beanlike subdomains probably account for the opening of the central aperture in the ligand-activated channel. The most pronounced motions in the TM domain are observed in the previously determined ryanodine-modified open channel (Fig. 4). The central opening in the transmembrane domain also appears to be larger in diameter (~18 Å) in the ryanodine-modified open state (Orlova et al., 1996).

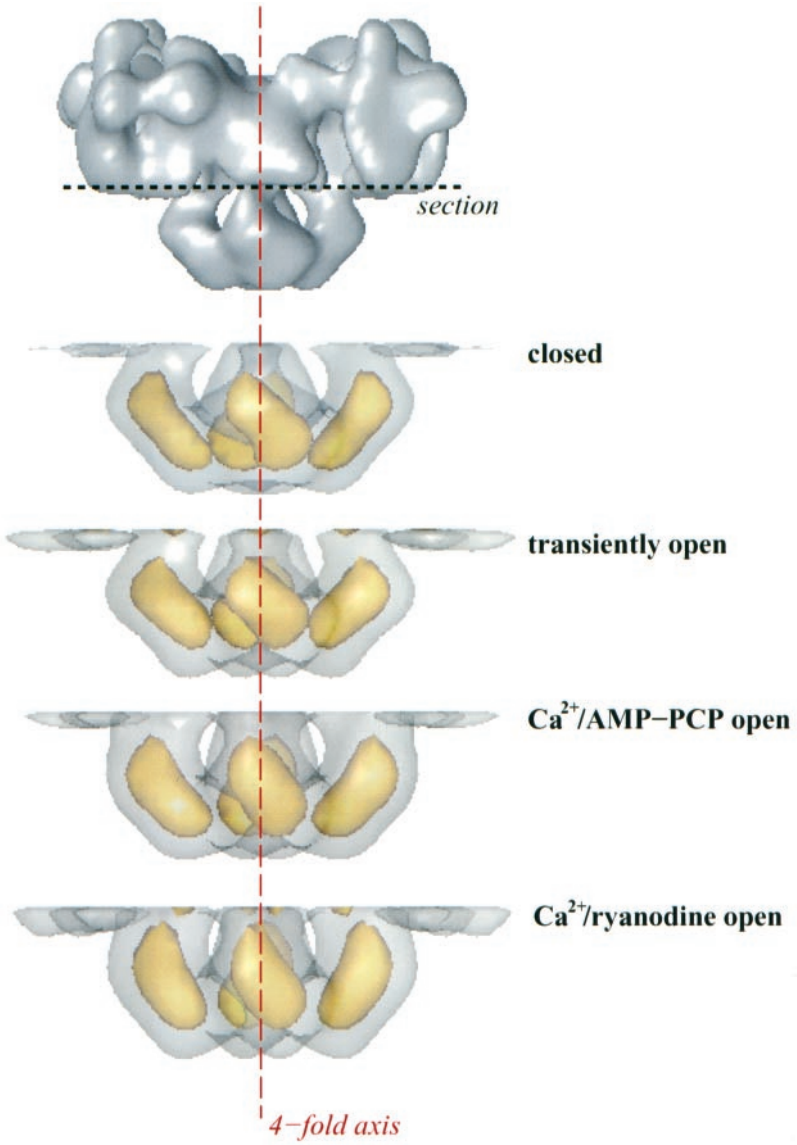

FIGURE 4 Comparison of transmembrane domains in three-dimensional maps of the skeletal muscle Ca^{2+} release channel in different functional states: closed, transiently open, Ca^{2+}/AMP-PCP open, open ryanodine-modified. For reference, the side view of the closed channel (*top*) is shown with the cytoplasmic face upward. The black dashed line denotes the level of section where reconstructions were cut perpendicular to the fourfold axis (*dashed line*). To emphasize the strongest differences between the maps, the transmembrane portion of the reconstructions, viewed in the direction normal to the fourfold axis, are shown at two different contour levels: the transparent surface encloses a 100% nominal molecular volume (mass of ~2.4 MDa), and the yellow surface 25%.

DISCUSSION

The SR Ca^{2+} release channel provides the pathway for the efflux of Ca^{2+} ions from the lumen of the SR during excitation-contraction coupling. Some Ca^{2+} release channels are probably opened in response to a change in the conformation of the voltage sensor in the transverse tubule membrane through a direct coupling mechanism (Rios and Brum, 1987). Other uncoupled channels may be activated by Ca^{2+} coming through the coupled channels (Escobar et al., 1994; Stern et al., 1997). Both the voltage sensor and Ca^{2+} probably interact with sites in the cytoplasmic domains of the Ca^{2+} release channel to regulate the opening of the cation-selective pore in the transmembrane domain (Du and MacLennan, 1998; Leong and MacLennan, 1998). Such regulatory mechanisms require long-distance allosteric changes in the structure of the Ca^{2+} release channel. Consistent with this, our work reveals significant conformational changes throughout the channel complex upon its activation with Ca^{2+} and AMP-PCP.

Long-range conformational changes in the transmembrane domain

The results of this study at 30-Å resolution highlight some elements of conformational changes in the quaternary architecture of the channel protein subunits. First, the reconstructions of the transiently open and the fully open channels indicate that the low-density region, seen at the center of the particles, is indeed a channel running through the whole structure along the fourfold axis, which opens into the SR lumen (Fig. 3 *c*). At the resolution of this study the actual size of the hole in the TM domain of the open channels cannot be determined with high accuracy, but the distinct funnel shape in the center of the TM domain shows substantial mass rearrangements upon channel activation. These observations support a model in which Ca^{2+} plays a role in triggering the opening of the gateway for Ca^{2+}. This opening may arise from the movements of the beanlike subdomains of the TM region of the channel in the different states (Fig. 4). Overall, the observed structural rearrange-

ments within the TM domain upon the activation of the Ca^{2+} release channel might be compared to the opening-closing of a camera diaphragm.

The opening of a central cavity in the transmembrane domain is seen upon activation of the channel by Ca^{2+}, Ca^{2+}/AMP-PCP, and Ca^{2+}/ryanodine. Ca^{2+}/ryanodine, however, appears to produce a larger "hole" (~18 Å) than is seen with Ca^{2+} or Ca^{2+}/AMP-PCP. Although it is difficult to assign significance to this size difference at our current resolution, it is possible that ryanodine also modifies the outer vestibule of the channel in the transmembrane domain, making it wider. The ryanodine-binding site is thought to be close to the C-terminal portion of the skeletal muscle Ca^{2+} release channel (Callaway et al., 1994; Witcher et al., 1994). It is not known, however, how ryanodine locks the channel in an open but reduced-conductance state. One possibility is that ryanodine binds within the open channel. Alternatively, its binding may allosterically regulate channel gating. In either case, the ryanodine-induced opening, triggered by binding close to or within the pore, may produce a different conformational change in the membrane-spanning domain than that triggered by the binding of some other modulator in the cytoplasmic domain. Consistent with this, a small vertical elongation of the channel, determined in the ryanodine-modified open channel (Orlova et al., 1996), was not seen in the presence of Ca^{2+} and AMP-PCP or Ca^{2+} alone. It seems possible that ryanodine binding to the high-affinity site(s) on the skeletal muscle Ca^{2+} release channel might induce additional mass movements in the transmembrane (~4° rotation) region and elongation of the channel (Orlova et al., 1996), thereby locking the channel in the steady open state.

Movements in the cytoplasmic region: implication for interaction with the voltage sensor

Another major change observed upon channel opening with Ca^{2+}/AMP-PCP is opening of the clamplike subdomains in the cytoplasmic region. The spacing of these structures is similar to that of the putative voltage sensors localized in the t-tubule above the skeletal muscle Ca^{2+}-release channel (Block et al., 1988). It is possible that these changes in the "clamps" regulate or are regulated by an interaction of the Ca^{2+} release channel with the voltage sensor. Because Ca^{2+} alone is not sufficient to maximally activate the channels (Copello et al., 1997), the closed clamp-shaped domains in the CY region in the transiently open state, compared to the fully open channel or the ryanodine-modified open channel (Orlova et al., 1996), may be due to averaging of a heterogeneous channel population as the channels are flickering between different gating modes. AMP-PCP and Ca^{2+} together produce a synergetic activation of the Ca^{2+} release channel by increasing the duration and frequency of open events and thereby driving the majority of the channels into a predominant functional state—the fully open state. However, we cannot eliminate the possibility that some of the channels could be desensitized (Ma, 1995). These conditions may not only trigger the opening of the channel, but could also affect its interaction with the t-tubule voltage sensor via a large conformational switch in the clamp-shaped domains. The coupling between the dihydropyridine receptor (DHPR) and the Ca^{2+} release channel is known to involve both orthograde (DHPR control of the Ca^{2+} release channel function) and retrograde (the Ca^{2+} release channel control of DHPR Ca^{2+} channel activity) coupling (Fleig et al., 1996; Nakai et al., 1996). The clamp domains may be involved in one or both of these interactions.

The results of this study support a model in which channel activation is associated with significant mass rearrangements in the channel complex, suggesting a highly allosteric regulation of channel opening. Further studies of the 3D architecture of the SR Ca^{2+} release channel at higher resolution under conditions where channel opening-closing can be controlled will undoubtedly strengthen the observations reported here and will result in more information concerning the molecular mechanism of ion translocation employed by the Ca^{2+} release channel.

We thank E. V. Orlova (Imperial College of Science, Medicine and Technology, London), S. Ludtke (Baylor College of Medicine, Houston), B. V. V. Prasad (Baylor College of Medicine, Houston, TX), L. Santacruz-Toloza (Baylor College of Medicine, Houston, TX), G. Rodney (Baylor College of Medicine, Houston, TX), and P. Moore (Baylor College of Medicine, Houston, TX) for helpful discussions.

This research is supported by grants from the National Institutes of Health (AR41729) and Muscular Dystrophy Association to SLH, the National Institutes of Health (RR02250) to WC, an EU grant (ERBI04-CT96-0592) to MvH, and a grant from American Heart Association (9730258N) to IIS.

REFERENCES

Block, B. A., T. Imagawa, K. P. Campbell, and C. Franzini-Armstrong. 1988. Structural evidence for direct interaction between the molecular components of the transverse tubule/sarcoplasmic reticulum junction in skeletal muscle. *J. Cell. Biol.* 107:2587–2600.

Callaway, C., A. Seryshev, J. P. Wang, K. J. Slavik, D. H. Needleman, C. Cantu, 3rd, Y. Wu, T. Jayaraman, A. R. Marks, and S. L. Hamilton. 1994. Localization of the high and low affinity [^{3}H]ryanodine binding sites on the skeletal muscle Ca^{2+} release channel. *J. Biol. Chem.* 269: 15876–15884.

Chu, A., M. Diaz-Munoz, M. J. Hawkes, K. Brush, and S. L. Hamilton. 1990. Ryanodine as a probe for the functional state of the skeletal muscle sarcoplasmic reticulum calcium release channel. *Mol. Pharmacol.* 37: 735–741.

Copello, J. A., S. Barg, H. Onoue, and S. Fleischer. 1997. Heterogeneity of Ca^{2+} gating of skeletal muscle and cardiac ryanodine receptors. *Biophys. J.* 73:141–156.

Coronado, R., J. Morrissette, M. Sukhareva, and D. M. Vaughan. 1994. Structure and function of ryanodine receptors. *Am. J. Physiol.* 266: C1485–C1504.

Diaz-Munoz, M., S. L. Hamilton, M. A. Kaetzel, P. Hazarika, and J. R. Dedman. 1990. Modulation of Ca^{2+} release channel activity from sarcoplasmic reticulum by annexin VI (67-kDa calcimedin). *J. Biol. Chem.* 265:15894–15899.

Du, G. G., and D. H. MacLennan. 1998. Functional consequences of mutations of conserved, polar amino acids in transmembrane sequences of the Ca^{2+} release channel (ryanodine receptor) of rabbit skeletal muscle sarcoplasmic reticulum. *J. Biol. Chem.* 273:31867–31872.

Escobar, A. L., J. R. Monck, J. M. Fernandez, and J. L. Vergara. 1994. Localization of the site of Ca^{2+} release at the level of a single sarcomere in skeletal muscle fibres. *Nature.* 367:739–741.

Fleig, A., H. Takeshima, and R. Penner. 1996. Absence of Ca^{2+} current facilitation in skeletal muscle of transgenic mice lacking the type 1 ryanodine receptor. *J. Physiol. (Lond.).* 496:339–345.

Fleischer, S., and M. Inui. 1989. Biochemistry and biophysics of excitation-contraction coupling. *Annu. Rev. Biophys. Biophys. Chem.* 18: 333–364.

Hawkes, M. J., M. Diaz-Munoz, and S. L. Hamilton. 1989. A procedure for purification of the ryanodine receptor from skeletal muscle. *Membr. Biochem.* 8:133–145.

Holmberg, S. R., and A. J. Williams. 1990. The cardiac sarcoplasmic reticulum calcium-release channel: modulation of ryanodine binding and single-channel activity. *Biochim. Biophys. Acta.* 1022:187–193.

Ikemoto, N., B. Antoniu, and L. G. Meszaros. 1985. Rapid flow chemical quench studies of calcium release from isolated sarcoplasmic reticulum. *J. Biol. Chem.* 260:14096–14100.

Jayaraman, T., A. M. Brillantes, A. P. Timerman, S. Fleischer, H. Erdjument-Bromage, P. Tempst, and A. R. Marks. 1992. FK506 binding protein associated with the calcium release channel (ryanodine receptor). *J. Biol. Chem.* 267:9474–9477.

Kang, J. J., A. Tarcsafalvi, A. D. Carlos, E. Fujimoto, Z. Shahrokh, B. J. Thevenin, S. B. Shohet, and N. Ikemoto. 1992. Conformational changes in the foot protein of the sarcoplasmic reticulum assessed by site-directed fluorescent labeling. *Biochemistry.* 31:3288–3293 (erratum: *Biochemistry.* 31:4922).

Lai, F. A., M. Misra, L. Xu, H. A. Smith, and G. Meissner. 1989. The ryanodine receptor-Ca^{2+} release channel complex of skeletal muscle sarcoplasmic reticulum. Evidence for a cooperatively coupled, negatively charged homotetramer. *J. Biol. Chem.* 264:16776–16785.

Leong, P., and D. H. MacLennan. 1998. The cytoplasmic loops between domains II and III and domains III and IV in the skeletal muscle dihydropyridine receptor bind to a contiguous site in the skeletal muscle ryanodine receptor. *J. Biol. Chem.* 273:29958–29964.

Ludtke, S., I. Serysheva, P. Baldwin, S. Hamilton, and W. Chiu. 1999. CTF corrected structure of the calcium release channel. *Biophys. J.* 76:A456.

Ma, J. 1995. Desensitization of the skeletal muscle ryanodine receptor: evidence for heterogeneity of calcium release channels. *Biophys. J.* 68:893–899.

Ma, J., M. Fill, C. M. Knudson, K. P. Campbell, and R. Coronado. 1988. Ryanodine receptor of skeletal muscle is a gap junction-type channel. *Science.* 242:99–102.

McGrew, S. G., C. Wolleben, P. Siegl, M. Inui, and S. Fleischer. 1989. Positive cooperativity of ryanodine binding to the calcium release channel of sarcoplasmic reticulum from heart and skeletal muscle. *Biochemistry.* 28:1686–1691.

Meissner, G. 1986a. Evidence of a role for calmodulin in the regulation of calcium release from skeletal muscle sarcoplasmic reticulum. *Biochemistry.* 25:244–251.

Meissner, G. 1986b. Ryanodine activation and inhibition of the Ca^{2+} release channel of sarcoplasmic reticulum. *J. Biol. Chem.* 261: 6300–6306.

Meissner, G. 1994. Ryanodine receptor/Ca^{2+} release channels and their regulation by endogenous effectors. *Annu. Rev. Physiol.* 56:485–508.

Meissner, G., E. Darling, and J. Eveleth. 1986. Kinetics of rapid Ca^{2+} release by sarcoplasmic reticulum. Effects of Ca^{2+}, Mg^{2+}, and adenine nucleotides. *Biochemistry.* 25:236–244.

Meissner, G., and A. el-Hashem. 1992. Ryanodine as a functional probe of the skeletal muscle sarcoplasmic reticulum Ca^{2+} release channel. *Mol. Cell. Biochem.* 114:119–123.

Meissner, G., and J. S. Henderson. 1987. Rapid calcium release from cardiac sarcoplasmic reticulum vesicles is dependent on Ca^{2+} and is modulated by Mg^{2+}, adenine nucleotide, and calmodulin. *J. Biol. Chem.* 262:3065–3073.

Nagasaki, K., and S. Fleischer. 1988. Ryanodine sensitivity of the calcium release channel of sarcoplasmic reticulum. *Cell Calcium.* 9:1–7.

Nakai, J., R. T. Dirksen, H. T. Nguyen, I. N. Pessah, K. G. Beam, and P. D. Allen. 1996. Enhanced dihydropyridine receptor channel activity in the presence of ryanodine receptor. *Nature.* 380:72–75.

Ogawa, Y. 1994. Role of ryanodine receptors. *Crit. Rev. Biochem. Mol. Biol.* 29:229–274.

Ohkusa, T., J. J. Kang, M. Morii, and N. Ikemoto. 1991. Conformational change of the foot protein of sarcoplasmic reticulum as an initial event of calcium release. *J. Biochem. (Tokyo).* 109:609–615.

Orlova, E. V., P. Dube, J. R. Harris, E. Beckman, F. Zemlin, J. Markl, and M. van Heel. 1997. Structure of keyhole limpet hemocyanin type 1 (KLH1) at 15 Å resolution by electron cryomicroscopy and angular reconstitution. *J. Mol. Biol.* 271:417–437.

Orlova, E. V., I. I. Serysheva, M. van Heel, S. L. Hamilton, and W. Chiu. 1996. Two structural configurations of the skeletal muscle calcium release channel. *Nature Struct. Biol.* 3:547–552.

Pessah, I. N., and I. Zimanyi. 1991. Characterization of multiple [^{3}H]ryanodine binding sites on the Ca^{2+} release channel of sarcoplasmic reticulum from skeletal and cardiac muscle: evidence for a sequential mechanism in ryanodine action. *Mol. Pharmacol.* 39:679–689.

Radermacher, M., V. Rao, R. Grassucci, J. Frank, A. P. Timerman, S. Fleischer, and T. Wagenknecht. 1994. Cryo-electron microscopy and three-dimensional reconstruction of the calcium release channel/ryanodine receptor from skeletal muscle. *J. Cell. Biol.* 127:411–423.

Rios, E., and G. Brum. 1987. Involvement of dihydropyridine receptors in excitation-contraction coupling in skeletal muscle. *Nature.* 325: 717–720.

Rousseau, E., J. Pinkos, and D. Savaria. 1992. Functional sensitivity of the native skeletal Ca^{2+}-release channel to divalent cations and the Mg-ATP complex. *Can. J. Physiol. Pharmacol.* 70:394–402.

Rousseau, E., J. S. Smith, and G. Meissner. 1987. Ryanodine modifies conductance and gating behavior of single Ca^{2+} release channel. *Am. J. Physiol.* 253:C364-C-368.

Sass, H. J., G. Buldt, E. Beckmann, F. Zemlin, M. van Heel, E. Zeitler, J. P. Rosenbusch, D. L. Dorset, and A. Massalski. 1989. Densely packed beta-structure at the protein-lipid interface of porin is revealed by high-resolution cryo-electron microscopy. *J. Mol. Biol.* 209:171–175.

Schatz, M., E. V. Orlova, P. Dube, J. Jager, and M. van Heel. 1995. Structure of *Lumbricus terrestris* hemoglobin at 30 Å resolution determined using angular reconstitution. *J. Struct. Biol.* 114:28–40.

Serysheva, I. I., E. V. Orlova, W. Chiu, M. B. Sherman, S. L. Hamilton, and M. van Heel. 1995. Electron cryomicroscopy and angular reconstitution used to visualize the skeletal muscle calcium release channel. *Nature Struct. Biol.* 2:18–24.

Smith, J. S., R. Coronado, and G. Meissner. 1986. Single-channel measurements of calcium release channel from skeletal muscle sarcoplasmic reticulum. *J. Gen. Physiol.* 88:573–588.

Smith, J. S., T. Imagawa, J. Ma, M. Fill, K. P. Campbell, and R. Coronado. 1988. Purified ryanodine receptor from rabbit skeletal muscle is the calcium-release channel of sarcoplasmic reticulum. *J. Gen. Physiol.* 92:1–26.

Stern, M. D., G. Pizarro, and E. Rios. 1997. Local control model of excitation-contraction coupling in skeletal muscle. *J. Gen. Physiol.* 110:415–440 (erratum: *J. Gen. Physiol.* 110:641).

Takeshima, H., S. Nishimura, T. Matsumoto, H. Ishida, K. Kangawa, N. Minamino, H. Matsuo, M. Ueda, M. Hanaoka, T. Hirose, et al. 1989. Primary structure and expression from complementary DNA of skeletal muscle ryanodine receptor. *Nature.* 339:439–445.

Timerman, A. P., E. Ogunbumni, E. Freund, G. Wiederrecht, A. R. Marks, and S. Fleischer. 1993. The calcium release channel of sarcoplasmic reticulum is modulated by FK-506-binding protein. Dissociation and reconstitution of FKBP-12 to the calcium release channel of skeletal muscle sarcoplasmic reticulum. *J. Biol. Chem.* 268:22992–22999.

Timerman, A. P., G. Wiederrecht, A. Marcy, and S. Fleischer. 1995. Characterization of an exchange reaction between soluble FKBP-12 and the FKBP.ryanodine receptor complex. Modulation by FKBP mutants deficient in peptidyl-prolyl isomerase activity. *J. Biol. Chem.* 270: 2451–2459.

Tinker, A., J. L. Sutko, L. Ruest, P. Deslongchamps, W. Welch, J. A. Airey, K. Gerzon, K. R. Bidasee, H. R. Besch, Jr., and A. J. Williams. 1996. Electrophysiological effects of ryanodine derivatives on the sheep

cardiac sarcoplasmic reticulum calcium-release channel. *Biophys. J.* 70:2110–2119.

van Heel, M. 1989. Classification of very large electron microscopical image data sets. *Optik.* 82:114–126.

van Heel, M., and G. Harauz. 1986. Resolution criteria for three dimensional reconstructions. *Optik.* 73:119–122.

van Heel, M., G. Harauz, and E. V. Orlova. 1996. A new generation of the IMAGIC image processing system. *J. Struct. Biol.* 116:17–24.

Wang, J. P., D. H. Needleman, and S. L. Hamilton. 1993. Relationship of low affinity [^{3}H]ryanodine binding sites to high affinity sites on the skeletal muscle Ca^{2+} release channel. *J. Biol. Chem.* 268:20974–20982.

Witcher, D. R., P. S. McPherson, S. D. Kahl, T. Lewis, P. Bentley, M. J. Mullinnix, J. D. Windass, and K. P. Campbell. 1994. Photoaffinity labeling of the ryanodine receptor/Ca^{2+} release channel with an azido derivative of ryanodine. *J. Biol. Chem.* 269:13076–13079.

Zhou, Z. H., S. Hardt, B. Wang, M. B. Sherman, J. Jakana, and W. Chiu. 1996. CTF determination of images of ice-embedded single particles using a graphics interface. *J. Struct. Biol.* 116:216–222.

Zhou, Z. H., B. V. Prasad, J. Jakana, F. J. Rixon, and W. Chiu. 1994. Protein subunit structures in the herpes simplex virus A-capsid determined from 400 kV spot-scan electron cryomicroscopy. *J. Mol. Biol.* 242:456–469.

Zorzato, F., J. Fujii, K. Otsu, M. Phillips, N. M. Green, F. A. Lai, G. Meissner, and D. H. MacLennan. 1990. Molecular cloning of cDNA encoding human and rabbit forms of the Ca^{2+} release channel (ryanodine receptor) of skeletal muscle sarcoplasmic reticulum. *J. Biol. Chem.* 265:2244–2256.